Understanding Near-surface and In-cloud Turbulent Fluxes in the Coastal Stratocumulus-topped Boundary Layers

Qing Wang
Meteorology Department, Naval Postgraduate School
Monterey, CA 93943
Phone: (831) 656-7716, Fax: (831) 656-3061 email: qwang@nps.edu

Award # N0001407WR20229

LONG-TERM GOAL

The long-term goal of this project is to understand the spatial and temporal variation of the surface fluxes in ocean upwelling coastal regions and to improve the physical parameterizations of surface flux and boundary layer processes in regional and climate models.

OBJECTIVES

The objective of this project is to understand the validity of bulk parameterizations of surface fluxes and the vertical structure of the marine atmospheric boundary layer (MABL) over the ocean in coastal regions where upwelling, swell and atmospheric dynamics such as expansion fans complicate the spatial and temporal variability of the turbulent fluxes. Our work in FY07 focused on a preliminary analysis of aircraft data collected during August 2006 in the framework of Adaptive Sampling And Prediction (ASAP) project. This data can be used to verify previous findings from similar data collected during Autonomous Ocean Sampling Network (AOSN-II) 2003 project.

APPROACH

Our analyses in the previous year (FY06) using AOSN-II data showed that longitudinal rolls are present in the marine boundary layer even at near-surface altitudes, which make cross wind sampling with aircraft preferable in order to avoid flux loss at large turbulence scales due to limited averaging length. Significant flux divergence due to incomplete mixing in the boundary layer was also observed especially in the case of heat (scalar) flux. Taking these effects into account, bulk estimates of turbulent transfer coefficients were in agreement with measured coefficients under unstable atmospheric conditions but not under stable conditions. The work in this year should verify these findings using the new ASAP data set and try to explain the behavior of drag coefficient at low wind speeds and turbulent heat transfer coefficient under stable conditions. Also dense soundings made at the north part of Monterey bay, where expansion fan phenomena were previously observed, are examined in order to understand the variation of the vertical structure of MABL in the along wind direction in this area.

Qing Wang is responsible for the overall project. Dr. John Kalogiros, an external research associate from National Observatory of Athens, Greece, works on the data analysis. In situ observations were made by the Twin Otter research aircraft operated by the Center for Interdisciplinary Remote Piloted Aircraft Studies (CIRPAS) at the Naval Postgraduate School (NPS) during the ASAP experiment.

Report Documentation Page

Form Approved
OMB No. 0704-0188

1. REPORT DATE	2. REPORT TYPE	3. DATES COVERED
30 SEP 2007	**Annual**	**00-00-2007 to 00-00-2007**

4. TITLE AND SUBTITLE	
Understanding Near-surface And In-cloud Turbulent Fluxes In The Coastal Stratocumulus-Topped Boundary Layers	5a. CONTRACT NUMBER
	5b. GRANT NUMBER
	5c. PROGRAM ELEMENT NUMBER
6. AUTHOR(S)	5d. PROJECT NUMBER
	5e. TASK NUMBER
	5f. WORK UNIT NUMBER
7. PERFORMING ORGANIZATION NAME(S) AND ADDRESS(ES) **Naval Postgraduate School,Meteorology Department,Monterey,CA,93943**	8. PERFORMING ORGANIZATION REPORT NUMBER
9. SPONSORING/MONITORING AGENCY NAME(S) AND ADDRESS(ES)	10. SPONSOR/MONITOR'S ACRONYM(S)
	11. SPONSOR/MONITOR'S REPORT NUMBER(S)

12. DISTRIBUTION/AVAILABILITY STATEMENT

Approved for public release; distribution unlimited

13. SUPPLEMENTARY NOTES

code 1 ony

14. ABSTRACT

The long-term goal of this project is to understand the spatial and temporal variation of the surface fluxes in ocean upwelling coastal regions and to improve the physical parameterizations of surface flux and boundary layer processes in regional and climate models.

15. SUBJECT TERMS

16. SECURITY CLASSIFICATION OF:			17. LIMITATION OF ABSTRACT	18. NUMBER OF PAGES	19a. NAME OF RESPONSIBLE PERSON
a. REPORT	b. ABSTRACT	c. THIS PAGE			
unclassified	**unclassified**	**unclassified**	**Same as Report (SAR)**	**9**	

Standard Form 298 (Rev. 8-98)
Prescribed by ANSI Std Z39-18

WORK COMPLETED

1. We performed a calibration of turbulence data (especially the wind turbulence radome probe) collected with the aircraft in order to check the stability and, thus, quality of the measurement systems.

2. We classified the flights based on average flow, we analyzed available flux profiles and calculated composite profiles based on MABL mixing.

3. We calculated spectra and neutral transfer coefficients and explained the issues left unresolved in AOSN-II data analysis.

4. We examined the vertical structure of MABL at the north part of Monterey bay during flow acceleration and turning at this region using dense sawtooth soundings (cross section).

RESULTS

Data preprocessing. ASAP aircraft data included eleven flights of CIRPAS Twin Otter aircraft in August 2006. The typical flight pattern was slightly different from those during AOSN-II experiment where no sounding legs were made and the surface legs shifted to more north latitudes (Figure 1a). On three flights (11th, 12th and 15th of August) low sawtooth soundings were made in a cross section parallel to the coast at the north of the Monterey Bay (Figure 1b). The flights took place in the morning (from 0930 to 1230 LST) at the same time period of day as most flights of AOSN-II.

The radome wind turbulence probe was calibrated using observations from the maneuver legs. The upwash effect, which is critical to the accuracy of the derived vertical wind velocity, was estimated. Minor differences from AOSN-II calibration were found within the possible error range. Fast radome data was sampled at 100 Hz and was sub-sampled to 20 Hz, which doubled the sampling frequency used in AOSN-II. This sampling frequency is sufficient to better resolve the inertial subrange of spectra of turbulent fluxes. Radome measurements were synchronized with other fast measurements and all data were quality controlled and noise removed in order to retrieve high-rate wind turbulence statistics.

(a) (b)

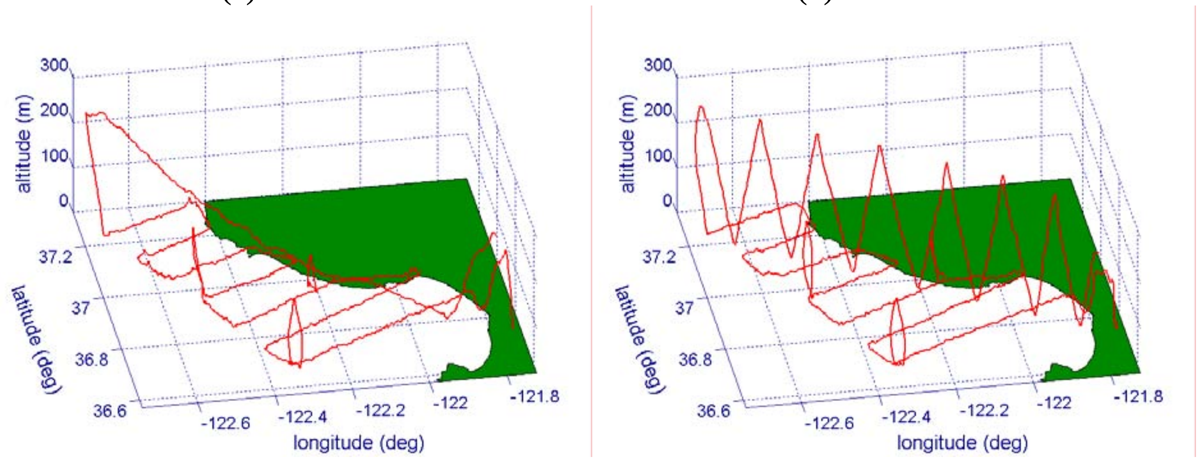

Figure 1: Flight tracks on (a) 8/2/2006 and (b) 8/11/2006.

Wind flow and MABL mixing categories. Flights were categorized based on average flow direction relatively to the coast and the presence of specific characteristics of the atmospheric flow such as wind acceleration at the northern part of Monterey Bay with possible expansion fan. Table 1 summarizes the classification of flights. The typical wind flow conditions, especially during summer, at the California coast are north-northwesterly wind along the coast which intensifies offshore. Half of ASAP data falls in this category with low to moderate wind speed that resulted in only minor wind acceleration in stead of an expansion fan at the north part of Monterey bay. The rest of the flights were made in westerly or southerly wind conditions with very low wind speed.

Table 1: Range of area averaged wind speed (U) and direction (dir) for each category of near sea surface atmospheric flow in the measurement region.

Flow Category	Date (August 2006)	U (m s^{-1})	dir (deg)
Northwesterly wind parallel to the coast	8, 9, 10, 11, 15	2.6-8.8	320-332
acceleration at north part of bay	8, 9, 11, 15	2.6-8.8	320-332
Southeasterly wind parallel to the coast	4, 5	2.5-2.8	124-133
Westerly onshore wind	2, 3, 7 , 12	2.2-3.4	239-289

Profiles of fluxes and mean quantities from aircraft soundings were analyzed in order to detect MABL mixing. Previous data analyses of profiles from AOSN-II experiment at the same time period of day had shown two categories of mixing in the area: well mixed (mixed up to the boundary layer height) and incomplete mixing (mixed up to half the boundary layer height) MABL as a possible result of morning destruction of stratocumulus in the area. Most cases belonged to the incomplete mixing categories. ASAP soundings were limited and only up to 200-300 m above sea surface (see Figure 1) compared to regular AOSN-II soundings with maximum altitude reaching 600 m.

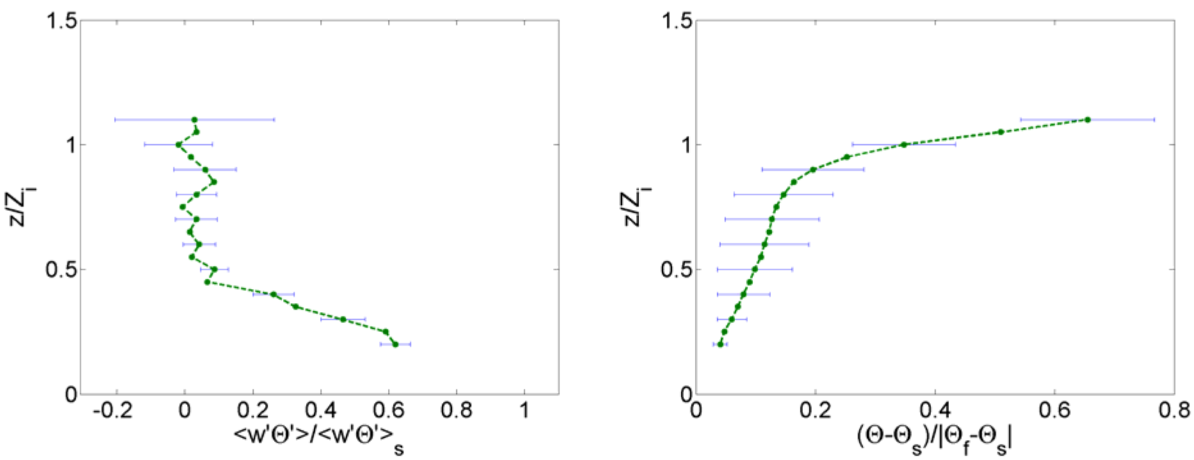

Figure 2: Average profiles with standard deviation of the mean of kinematic heat flux $<w'\Theta'>$ normalized with near surface value $<w'\Theta'>_s$ and potential temperature normalized with near surface Θ_s and free atmosphere Θ_f for cases of not well mixed boundary layer.

Available ASAP profiles showed similar behavior but with very few well mixed MABL cases. Figure 2 shows composite (average of similar cases) profiles of heat flux and potential temperature from incomplete mixing MABL cases. Turbulent flux is close to zero at half the boundary layer height Z_i defined as the base of temperature inversion capping the MABL and potential temperature has a small positive gradient in the boundary layer.

Turbulent flux spectra and transfer coefficients. We computed the power spectra of fast sampled turbulent quantities (wind velocity components, temperature and water vapor mixing ratio) and co-spectra of turbulent fluxes using 10 km averaging legs. Composite normalized spectra were then computed for different atmospheric stabilities based on stability parameter z/L (z is the measurement altitude and L is the Monin-Obukhov length). Figure 3 shows composite co-spectra of along average wind momentum flux. Typical similarity functions (e.g., G(z/L)) were used in the normalization. Frequency f was normalized with z and airspeed U_a. Separate spectra were estimated for along and cross wind sampling directions. It is found that longitudinal rolls, which are present in MABL even close to sea surface, shift turbulent energy to higher frequency in the cross wind sampling. This conclusion is similar to that obtained from the AOSN-II dataset. With the higher sampling frequency compared to AOSN-II, the ASAP spectra show that the inertial subrange extends well up to the Nyquist frequency. However, lower energy at low frequencies is observed compared to similarity spectra in the along wind sampling, while AOSN-II dataset showed better consistency. We note that AOSN-II dataset included four times more flights and more data per flight due to longer duration of each flight. Thus, AOSN-II quantitative statistics are probably more reliable compared to ASAP data.

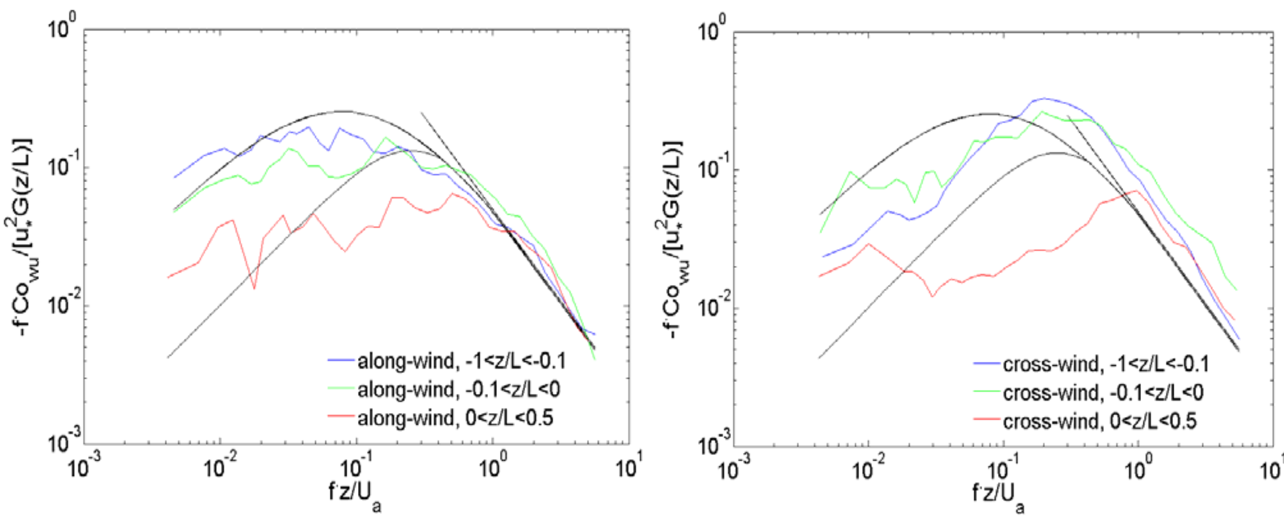

Figure 3: Composite (average) normalized spectra of along wind momentum -<w'u'> in along and cross wind sampling directions and 10 km legs averaging. Bulk estimates of fluxes were used for spectra normalization Similarity spectra for unstable and stable conditions and inertial subrange are shown with black lines.

Turbulent transfer coefficients were computed and reduced to neutral conditions and 10 m altitude above sea surface using similarity functions similar to those used in bulk algorithms such as COARE 3.0. Figure 4 shows drag and heat transfer neutral coefficients against wind speed for unstable atmospheric conditions. Unfortunately, very few cases with stable atmospheric conditions were observed in ASAP to give reliable results over a significant range of wind speed values. Thus, the higher sampling frequency compared to AOSN-II, which was intended to benefit reliable estimation of turbulent fluxes under stable conditions characterized by smaller turbulence scales compared to unstable ones, was not fully utilized.

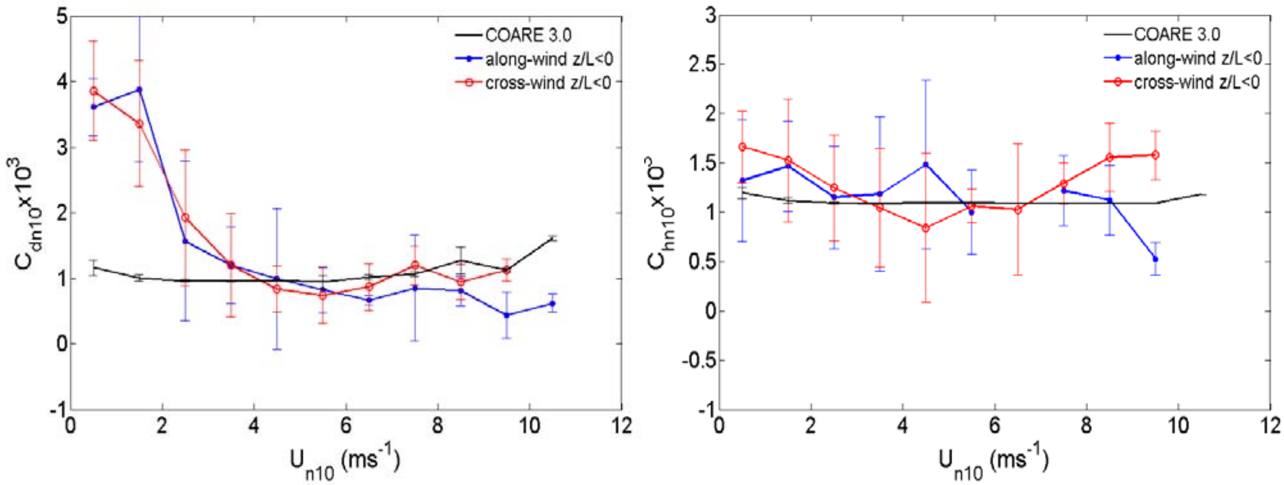

Figure 4: Momentum (C_{dn10}) and heat (C_{hn10}) flux transfer coefficients for unstable atmospheric conditions (z/L<0) after flux divergence correction against wind speed (U_{n10}) at 10 m AMSL.

Flux divergence correction was applied to turbulent fluxes based on the average divergence observed in the composite flux profiles. Along- wind sampling gives lower turbulent transfer coefficients compared to cross wind sampling at wind speed of about 8 ms^{-1} or higher. At low wind, drag coefficients are much higher compared to bulk estimates (COARE 3.0). Similar results were obtained from the AOSN-II dataset.

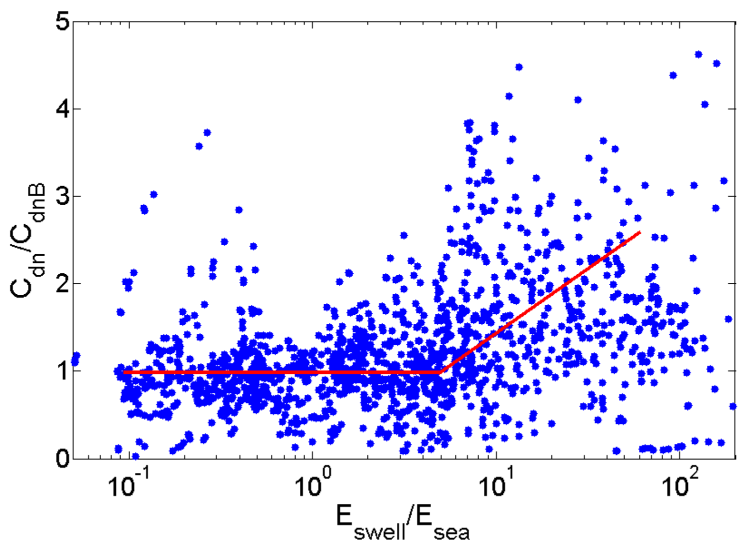

Figure 5: Ratio of measured (C_{dn}) in cross wind sampling (corrected for flux divergence) and bulk estimated (C_{dnB}) drag coefficient for unstable atmospheric conditions against the ratio of swell to sea wave energy using AOSN-II data. Wave data from NDBC buoy 46028 (longitude -122.42°, latitude 36.75°) were adjusted with locally measured wind and wave heights.

We also re-examined the causes of high drag coefficients under all atmospheric stabilities and the decreasing of heat transfer coefficient under stable conditions at low wind speeds using AOSN-II data.

Because direct wave measurements were not available, we estimated swell and sea wave parameters at each measurement location with the aircraft using wave data from NDBC buoy 46028 (longitude -122.42°, latitude 36.75°), which were adjusted with locally measured wind and wave height using relations from available literature. Figure 5 shows the ratio of measured to bulk estimated neutral drag coefficient at 10 m above sea level against swell to sea energy. It is found that the swell effect is significant at energy ratios above 5, which is in agreement with previous literature. We hence confirm that the high values of drag coefficient at low winds (where swell dominates sea energy) are due to swell effects.

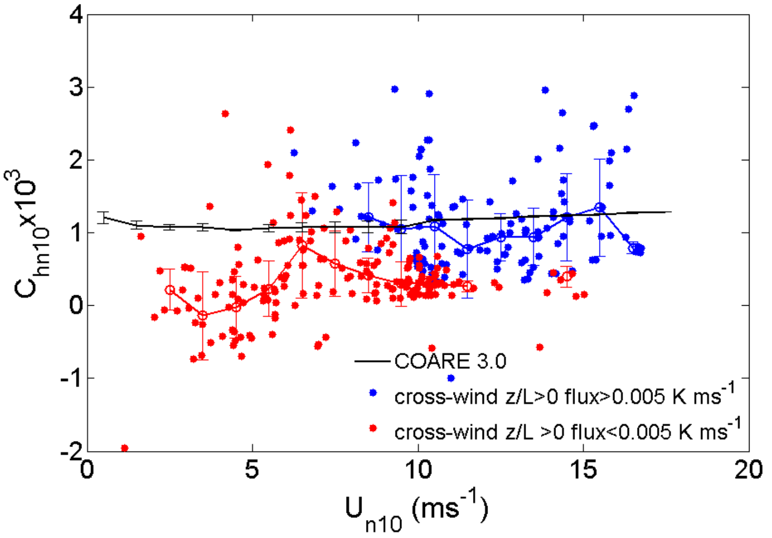

Figure 6: Heat (C_{hn10}) flux transfer coefficient for stable atmospheric conditions (z/L>0) and cross-wind sampling after flux divergence correction against wind speed (U_{n10}) at 10 m AMSL using AOSN-II data.

Figure 6 shows the heat transfer coefficient under stable atmospheric conditions from AOSN-II dataset corrected for flux divergence using composite profiles divergence. The data were separated into two categories: low flux and high flux cases. To avoid significant measurement errors and errors introduced by flux divergence, data with large air-sea temperature difference or when z/Z_i is greater than 0.5 were excluded from Fig. 6. Figure 6 shows that cases with large heat flux resulted in transfer coefficients that are consistent with the COARE bulk estimates. The small heat fluxes could probably induce large errors in estimated transfer coefficients due to measurement error, which may also result in the negative transfer coefficients.

Horizontal and vertical MABL structure. Figures 7 and 8 show the spatial and vertical variations of wind, SST, surface stress and stress curl during an event with moderate northwesterly wind (11/8/2006). On this day, a moderate acceleration and turning of wind and a moderate cool upwelling pool at the north part of Monterey bay were observed (Figure 7). Wind stress curl, which was estimated from wind stress field interpolated on a regular grid with 5 km resolution, shows a clearly positive, although not large in magnitude, value in the upwelling area. This is in agreement with the conclusion from the AOSN-II dataset that large coherent areas of positive curl of wind stress coincide with upwelling areas in the coastal zone.

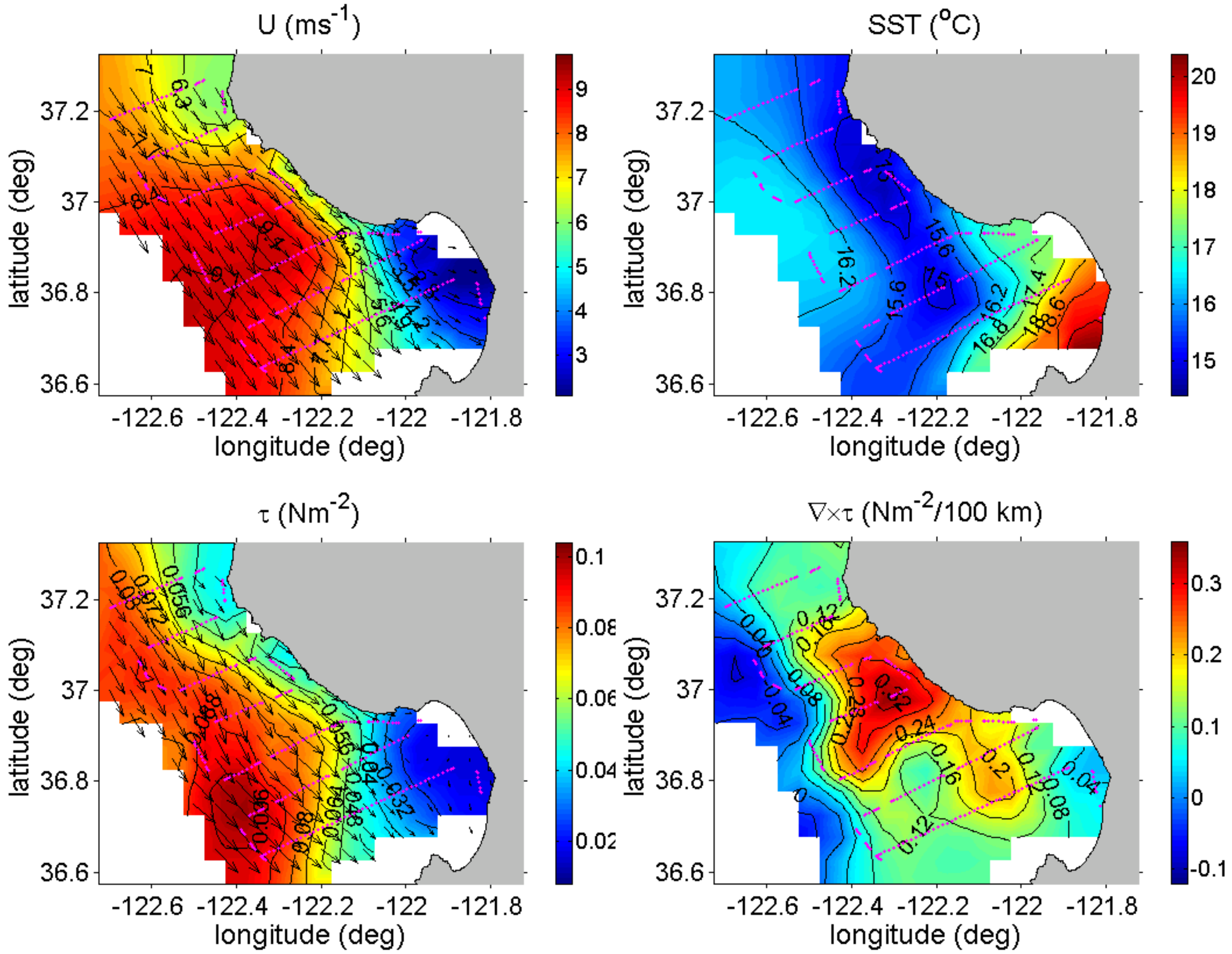

Figure 7: Spatial distribution of wind speed (U), SST, wind stress (τ), and wind stress curl (∇ x τ) estimated from aircraft legs at about 35 m above sea level on August 11, 2006 from about 0928 to 1117 LST. Purple points are the positions of the 5 km legs used for generating the plots.

Figure 8 shows the low-level vertical cross section at the north part of Monterey bay using the sawtooth soundings shown in Figure 1b. These dense soundings give a detailed cross section following the moderate acceleration of wind speed in this area. It is seen here that wind acceleration is limited in the MABL and its height becomes lower in the region of wind acceleration followed by rapid increases downwind in the bay where wind slows down. Weak turbulence is observed in regions of low boundary layer height. The lowering of temperature inversion at this area is also combined with drier air from the free atmosphere. These findings agree with characteristics of expansion fans described in the literature and, thus, confirm that events with large wind speed acceleration in this area observed in AOSN-II dataset (but cross section were not available) were the result of expansion fans.

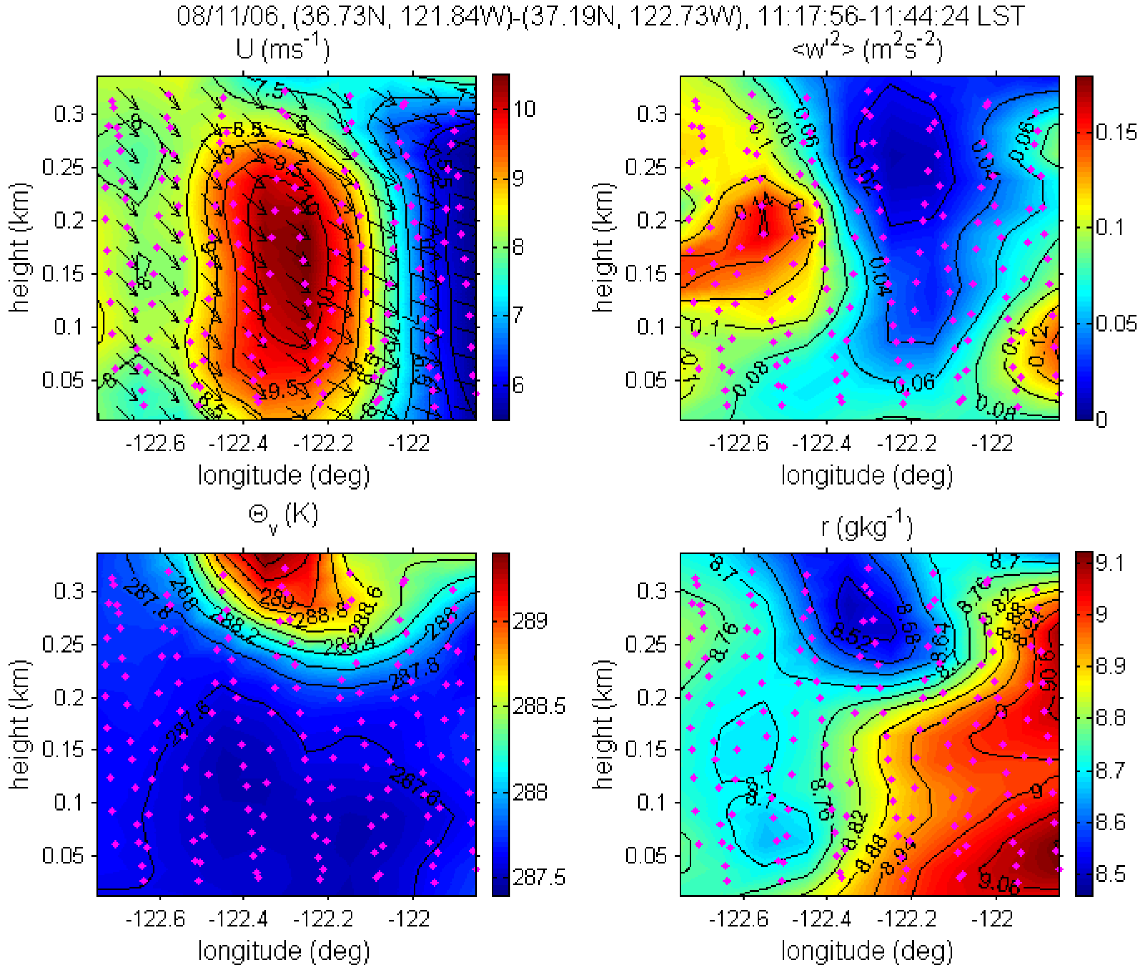

Figure 8: Cross sections of wind speed (U), virtual potential temperature (Θ_v), vertical velocity variance ($<w'^2>$, 500 m horizontal averaging legs) and water vapor mixing ratio (r) using the sawtooth soundings on 8/11/2006 (see Fig. 1). Purple dotted lines denote the flight tracks used to generate the plots.

IMPACT/APPLICATIONS

Our observational analysis of ASAP 2006 data verified the characteristics of MABL observed in AOSN-II: longitudinal rolls effects reaching to the sea surface, incomplete mixing of atmospheric boundary layer, coincidence of positive wind stress curl with upwelling regions, and frequent expansion fan at the north part of Monterey bay under northwesterly wind. These finding will help in more accurate evaluation of turbulence parameterizations in coastal atmospheric boundary layers coupled with ocean upwelling.

TRANSITIONS

The results of this project will potentially help to understand the MABL structure and evaluate and improve the turbulence parameterizations of mesoscale models in the complex coastal zone.

RELATED PROJECTS

Related project is the CBLAST project for surface flux parameterization (ONR award to NPS # N0001407WR20228 and ONR award to NRL # N0001407WX20972).

PUBLICATIONS

Wang, Q., J. Kalogiros, S. Ramp, J. Paduan, G. Buzorius and H. Jonsson, (2007): Wind stress and local upwelling in the Monterey Bay observed during AOSN-II. Submitted to *J. Geophys. Res.,* in revision.

Kalogiros, J., and Q. Wang, (2007): Aircraft observations of near sea surface turbulence fluxes in the coastal zone. In preparation for submission to *Boundary-Layer Meteorology*.